Journal of The Electrochemical Society, **153** (11) F249-F254 (2006)
0013-4651/2006/153(11)/F249/6/$20.00 © The Electrochemical Society

Metallorganic Chemical Vapor Deposition of Hafnium Silicate Thin Films Using a Dual Source Dimethyl-alkylamido Approach

Steven Consiglio,[a] Filippos Papadatos,[a] Sebastian Naczas,[a] Spyridon Skordas,[b] Eric T. Eisenbraun,[a] and Alain E. Kaloyeros[a]

[a]*College of Nanoscale Science and Engineering, The State University of New York at Albany, Albany, New York 12203, USA*
[b]*IBM Microelectronics, Hopewell Junction, New York 12533, USA*

A low-temperature metallorganic chemical vapor deposition process has been developed for the growth of hafnium silicate thin films for advanced gate dielectric applications. In this process, a metallorganic hafnium precursor, tetrakis(dimethylamino-)hafnium, and a metallorganic silicon precursor, tris(dimethylamino)silicon, were employed, using O_2 as a co-reactant. Films were deposited at a substrate temperature in the range of 250–450°C. The films were subsequently annealed in oxygen and forming gas ambients to assess thermal stability. The resulting films were characterized by Auger electron spectroscopy to determine composition and X-ray diffraction to determine microstructure. Electrical test structures were fabricated with as-deposited and annealed hafnium silicate films, and C-V and J-V measurements were performed. As-deposited dielectric constant values ranging from 6.9 to 12.9 were achieved depending on processing conditions and resulting film composition. Leakage current density at flatband voltage minus 1 V for a 26 nm thick as-deposited film was measured to be 1.6×10^{-1} A/cm^2 and was shown to decrease following an O_2 anneal. The performance of these hafnium silicate films was also compared to hafnium oxide films deposited using the same Hf precursor and O_2 oxidizer approach.
 [DOI: 10.1149/1.2338634]

Manuscript submitted May 10, 2006; revised manuscript received July 11, 2006. Available electronically September 6, 2006.

For future generations of complementary metal-oxide semiconductor (CMOS) devices, a new insulating material is required to replace SiO_2, which suffers from high leakage current and reliability issues as the physical thickness scales below ~1.5 nm.[1] A number of high dielectric constant metal oxide materials such as HfO_2, ZrO_2, Y_2O_3, and La_2O_3 are being considered for next generation gate dielectric applications.[2] However, these simple "unary" metal oxide materials have been shown to undergo thermally induced crystallization at typical post-dielectric deposition processing temperatures, which can be problematic due to the possibility of increased leakage current and dopant diffusion across the dielectric grain boundaries,[3] as well as threshold voltage instability as a result of charge trapping.[4,5] One approach to overcoming these difficulties is to incorporate a silicate phase material into the metal oxide matrix, which lowers the overall dielectric constant but results in an amorphous microstructure with enhanced phase stability and lower trap densities as compared to the simple metal oxide counterparts. Among all the pseudo-binary phases of the aforementioned metal oxides, hafnium silicate is currently one of the leading candidates for a replacement gate dielectric scheme, given the combination of attractive properties that HfO_2 possesses. These include a high dielectric constant (21-25), good thermodynamic stability on Si,[6] a large band gap (~5.7 eV), and reasonable conduction band offset to Si (1.4 eV).[7]

For the deposition of a multicomponent film, chemical vapor deposition (CVD) is an attractive process because film properties and stoichiometry can be tailored via simple changes to the processing parameters. In particular, the use of liquid metallorganic sources, as opposed to solid inorganic halide containing sources, is desirable for gate dielectric CVD processes to avoid the incorporation of corrosive contaminants in the process environment, which is considered to be problematic for microelectronic applications.[8] For CVD of group IVB oxides, metal alkylamide precursors have desirable properties for implementation in a manufacturing environment. Specifically, recent studies have shown promising results for the precursors tetrakis(dimethylamino)hafnium $Hf[N(CH_3)_2]_4$,[9-13,23] tetrakis(diethylamino)hafnium $Hf[N(C_2H_5)]_4$,[13-20,23] and tetrakis(ethylmethylamino)hafnium $Hf[N(CH_3)(C_2H_5)]_4$[11,21-23] used for the growth of HfO_2 thin films. These precursors are typically liquids at room temperature and have sufficient vapor pressures and decomposition characteristics that are appropriate for CVD processing, with the dimethyl derivative exhibiting the highest volatility (vapor pressure of 1 Torr at 75°C as compared to 1 Torr at 113°C and 1 Torr at 126°C for the diethyl and ethylmethyl derivatives, respectively).[23]

Another benefit of using a dialkylamide hafnium precursor is the existence of chemically compatible silicon dialkylamide precursors for the growth of hafnium silicate materials. This is important when employing simultaneous delivery of precursor sources to the processing chamber to avoid potential issues associated with ligand exchange between the different sources and undesirable gas-phase reactions in the delivery zone. The silicon sources tetrakis(dimethylamino)silane $Si[N(CH_3)]_4$ and tris(dimethylamino)silane $SiH[N(CH_3)]_3$ have been previously studied for the growth of silicon based dielectrics in CVD processes.[24-28] These precursors are both liquids at room temperature and also possess sufficient volatility for CVD manufacturing with the tris-dimethyl precursor having the higher volatility (vapor pressure of 9.3 Torr at 30°C as compared to 2.8 Torr at 30°C for the tetrakis-dimethyl precursor).[29]

In this paper, we present results using tetrakis(dimethylamino) hafnium (TDMAH) and tris(dimethylamino)silicon (TDMAS) as the Hf and Si source, respectively, with O_2 as the oxidizing co-reactant, in a metallorganic chemical vapor deposition (MOCVD) process. The electrical properties and microstructural stability of the resulting films were assessed by ex situ postdeposition annealing in both oxidizing and reducing ambients. Hafnium silicate films were also compared to hafnium oxide films deposited using the same Hf precursor and O_2 oxidizer approach with respect to electrical performance and stability.

Experimental

CVD processing.— For all depositions, a stainless steel 200 mm wafer capable warm-wall CVD chamber was utilized. The processing chamber was connected to a high vacuum loadlock for wafer transport and handling. Both precursor sources were loaded in separate stainless steel bubblers in an inert ambient glovebox. The bubblers were attached to separate delivery lines equipped with individual MKS Instruments type 1153A vapor source delivery systems, which were used for accurate control of precursor flows without the need for carrier gas. The two precursor delivery lines were merged in a common delivery inlet at the top of the process chamber. The bubbler containing the TDMAH precursor was heated to ~70°C for all the depositions, while the TDMAS precursor bubbler was left at room temperature due to the high vapor pressure of that source. To prevent precursor condensation, the delivery lines for the precursor

Table I. Summary of processing parameters used for MOCVD growth of Hf silicate films.

Substrate temperature	250–450°C
O_2 flow rate	300 sccm
$Hf(NMe_2)_4$ flow rate	1 sccm
$SiH(NMe_2)_3$ flow rate	10 sccm
Ar flow rate	50 sccm
Pressure	1 Torr

sources and the MKS type 1153A units were kept at temperatures of 60 and 75°C for the Si and Hf source delivery lines, respectively.

The substrate used for the depositions was p-type Si (100), which was loaded on a Mo carrier wafer and transported into the process chamber via the loadlock using a robotic arm. The substrates were dipped in dilute HF solution followed by a rinse in deionized water and a N_2 gas drying step to remove any native oxide prior to introduction into the process chamber. After the wafer was loaded into the loadlock and the loadlock was evacuated, the wafer was moved to the resistively heated wafer chuck in the process module. A flow of 50 sccm of Ar was provided to the back side of the wafer chuck to achieve uniform heat distribution and to provide diluent gas to help set the process pressure, which was maintained by the use of an actively controlled exhaust throttle valve.

Prior to the run, the precursor flow from both sources was stabilized by flowing through a line which bypassed the deposition chamber and was routed directly to the pump stack. Each deposition was initiated by simultaneous introduction of Hf precursor, Si precursor, and O_2 into the process chamber. The substrate temperature range investigated was 250–450°C. The flow rates used for the Hf precursor, Si precursor, and O_2 were fixed at 1, 10, and 300 sccm, respectively, while the process pressure was fixed at 1 Torr. These baseline process conditions were based on results from initial screening experiments for HfO_2 growth carried out in the same processing tool without the addition of the Si source. All reactants were introduced coincidentally so as to minimize potential parasitic silicon oxide growth prior to the CVD growth. A summary of the key parameters used for these depositions is displayed in Table I.

Thermal post-processing.— The as-deposited films were annealed ex situ in both oxidizing and reducing ambients to assess thermal stability and both chemical and electrical changes. The oxidizing ambient used was O_2 (purity 99.5%) at a temperature of 700°C at 700 Torr for 1 h. The reducing ambient used was forming gas (95% Ar, 5% H_2) at temperatures of both 500 and 700°C at 700 Torr for 1 h.

Characterization Techniques.— The resulting films were characterized by Auger electron spectroscopy (AES) to determine chemical composition, X-ray diffraction (XRD) to investigate microstructure, scanning electron microscopy (SEM) to measure film thickness, and capacitance-voltage (C-V) and current density-voltage (J-V) measurements to investigate key electrical properties such as dielectric constant and leakage current performance.

AES measurements were performed using a PHI 600 system with a LaB_6 electron source operating at a primary beam energy of 5 keV and 1 μA. Compositional depth profiling was performed by sputter etching using 3 keV Ar^+ ions followed by subsequent data collection for each sputter cycle. XRD was performed using a Scintag XDS 2000 in which X-rays were generated using a Cu Kα X-ray source at 40 mA and 45 kV. SEM measurements were performed using a Zeiss/LEO model 1550 field-emission microscope operating with a primary beam voltage of 5 kV. Electrical measurements were performed on MIS capacitor structures fabricated using Al electrodes with an area of 7.85×10^{-3} cm^2 sputter deposited through a shadow mask on the wafer front side and blanketwise on the wafer back side, after a receiving a dilute HF clean, to ensure robust electrical contact. C-V and J-V measurements were performed using a MDC model DG8 electrical characterization probe station, equipped with a HP4284 precision LCR meter and a HP4140B dc pA-meter for capacitance and current measurements, respectively.

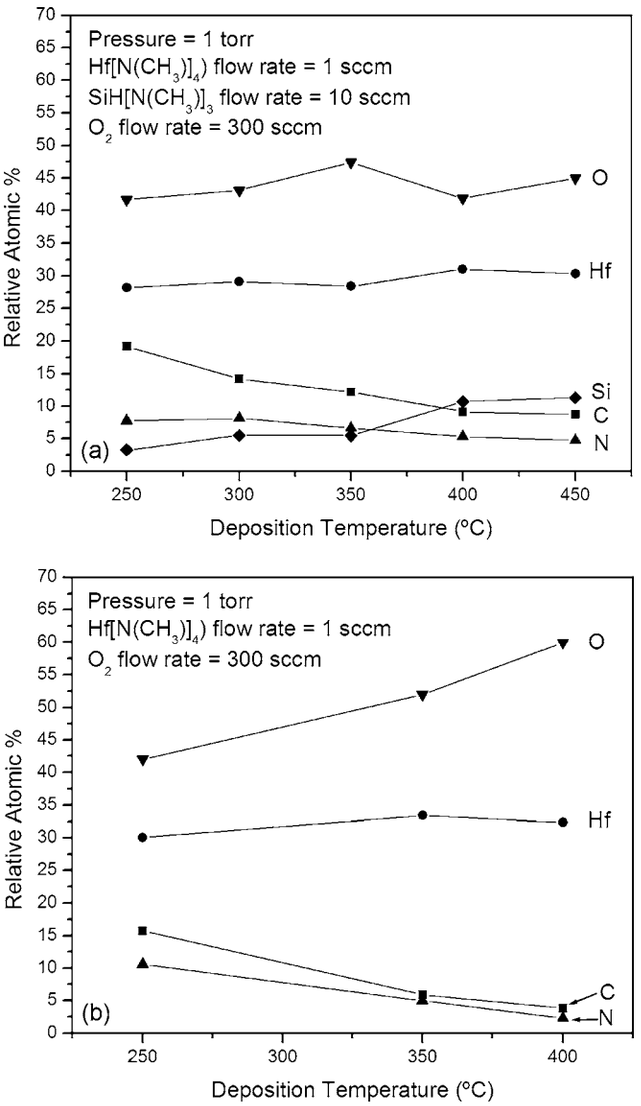

Figure 1. Relative atomic concentrations of (a) C, N, Si, Hf, and O for Hf silicate films as a function of deposition temperatures and (b) C, N. Hf, and O for HfO_2 films as a function of deposition temperature.

Results and Discussion

Composition.— Figure 1a shows the results of AES measurements of the levels of C and N impurities, and Hf, Si, and O relative atomic percentage in the film matrix, as a function of deposition temperature. The films in this study ranged in thickness from 30–200 nm. In particular, at deposition temperatures below 350°C, less than 6 atom % Si incorporation is observed, and the amounts of C and N impurities are >10 and ~6 atom %, respectively. Above 350°C, increased Si incorporation is observed, while the amount of incorporated C and N decreases. However, the C and N levels observed are above the levels observed in CVD-grown HfO_2 films deposited at the same temperature, flow, and pressure conditions using the same tetrakis(dimethylamino)hafnium and O_2 chemistry without the addition of tris(dimethylamino)silane, as shown in Fig. 1b for reference. This suggests that the additional C and N impurities are due to the addition of the Si precursor, and that at tempera-

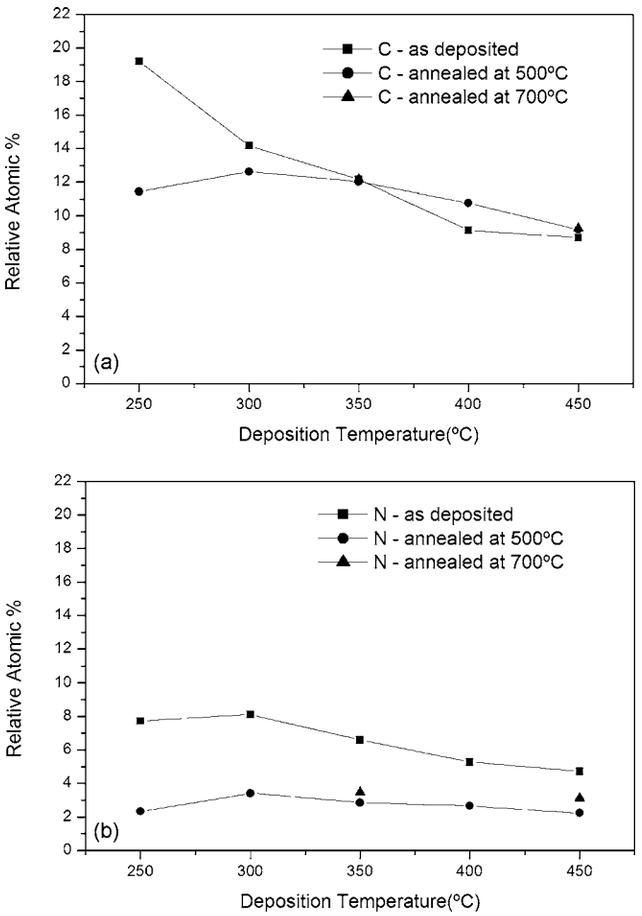

Figure 2. Relative atomic concentrations before and after forming gas annealing of (a) C for Hf silicate films as a function of deposition temperature and (b) N for Hf silicate films as a function of deposition temperature.

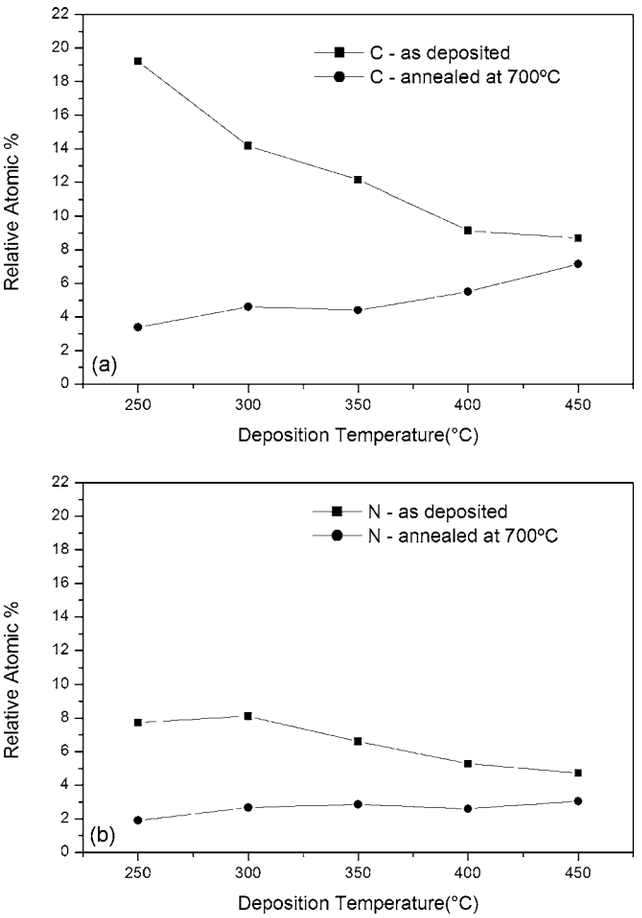

Figure 3. Relative atomic concentrations before and after O_2 annealing of (a) C for Hf silicate films as a function of deposition temperature and (b) N for Hf silicate films as a function of deposition temperature.

tures below 350°C there is insufficient thermal energy to lead to a clean decomposition of the Si source, resulting in the growth of a contaminated hafnium silicate phase.

If these contaminants are due to incorporated amido ligand fragments, it should be possible to remove these contaminants via thermal postprocessing. In this respect, Fig. 2a and b display the levels of C (Fig. 2a) and N (Fig. 2b) for each deposition temperature after annealing in forming gas ambient at 500 and 700°C. As can be seen, there is a decrease in N levels following forming gas ambient anneal while C levels remain relatively constant after annealing. Likewise, Fig. 3a and b show the levels of C and N for all deposition temperatures following a postdeposition O_2 annealing step at 700°C. A decrease in both C and N levels after annealing, and an overall increase in postannealing C and N levels with increasing deposition temperature is observed, in contrast with the reduction in contamination measured for as-deposited samples as deposition temperature is increased. These trends suggest two different phases of material being deposited at low deposition temperature and high deposition temperature processing regimes, which correlates with the different observed level of Si incorporation as a function of deposition temperature.

Microstructure.— Figure 4 shows the XRD 2θ scan for 30–200 nm thick films deposited in the substrate temperature range of 250–450°C. The absence of peaks suggest an amorphous microstructure for the as-deposited films. Likewise, Fig. 5a and b show the XRD 2θ scan for films annealed at 700°C in forming gas and O_2 ambients, respectively, suggesting that the amorphous phase is maintained after the anneals. By comparison, a 50 nm CVD grown HfO_2 films deposited using tetrakis(dimethylamino)hafnium with O_2 as a co-reactant exhibited crystallization of the monoclinic phases

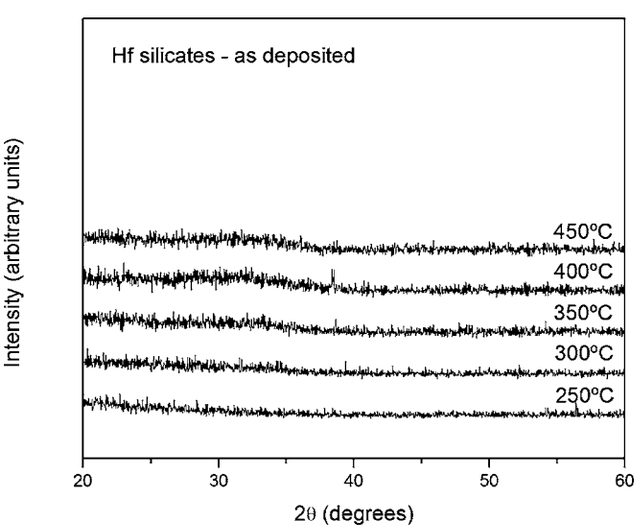

Figure 4. XRD 2θ scans for as deposited Hf silicate films.

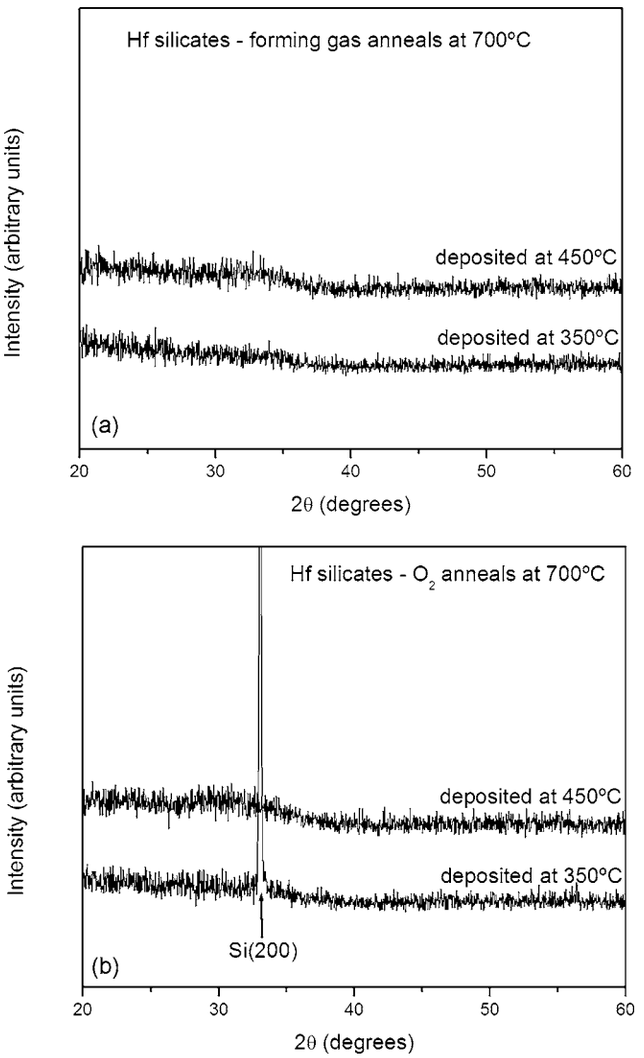

Figure 5. XRD 2θ scans for Hf silicate films deposited at 350 and 450°C after annealing in (a) forming gas ambient at 700°C and (b) O_2 ambient at 700°C.

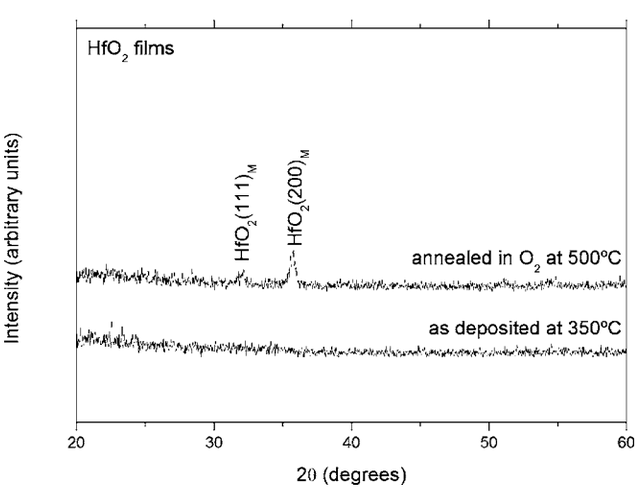

Figure 6. XRD 2θ scans for as-deposited HfO_2 film and after annealing in O_2 ambient at 500°C showing crystallization of the monoclinic phases.

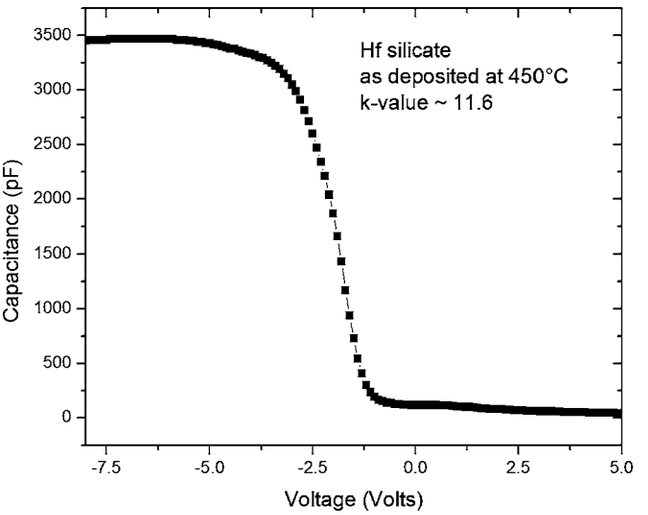

Figure 7. Representative C-V plot, measured at 100 kHz, of a Hf silicate film deposited at 450°C.

following an O_2 anneal at only 500°C, as shown in Fig. 6. These results confirm that the incorporation of Si in these metallorganic CVD-grown films results in higher stability of the amorphous phase, which is consistent with the behavior observed for $HfSi_xO_y$ films deposited using other techniques.[30,31]

Electrical properties.— Figure 7 shows a representative C-V plot, measured at 100 kHz, employing a 26 nm thick Hf silicate film deposited at 450°C. The C-V data shows clear accumulation, depletion, and inversion regions and a flatband voltage of −1.0 V. A portion of this negative shift in flatband voltage can be attributed to the large work function difference between the Al electrode and the Si substrate (~0.6 eV), assuming work functions of 4.3 and 4.9 eV, respectively, while the additional negative flatband voltage shift suggests the presence of positive net charge in the oxide. From the measured accumulation capacitance, the effective dielectric constant was calculated to be 11.6. In comparison, the effective dielectric constant of a 26 nm thick MOCVD-grown HfO_2 film deposited at 350°C was determined to be 13, which is expected given the absence of silicon incorporation. Table II summarizes the effective dielectric constant values measured for the as-deposited and annealed films deposited at 350 and 450°C. It can be seen that the dielectric constant is strongly dependent both upon deposition temperature as well as annealing conditions.

Likewise, Fig. 8a-c display J-V measurements for a representative as-deposited 26 nm thick Hf silicate film deposited at 450°C (Fig. 8a), and the same sample after annealing in forming gas (Fig. 8b) and O_2 ambients (Fig. 8c). Values for leakage current density at flatband voltage minus 1 V (V_{FB}-1) are inset in these figures. From these results, we see a decrease in leakage current density following annealing with the lowest value observed following the O_2 annealing. This 5000 times reduction may be due to the growth of an interfacial oxide phase, which is also suggested by the decrease in effective dielectric constant following the O_2 anneal. In comparison,

Table II. Summary of effective dielectric constant values measured for the as-deposited and annealed Hf silicate films deposited at 350°C and 450°C.

	350°C deposition	450°C deposition
As-deposited	6.9	11.6
Forming gas annealed at 700°C	7.3	12.9
O_2 annealed at 700°C	9.1	9.1

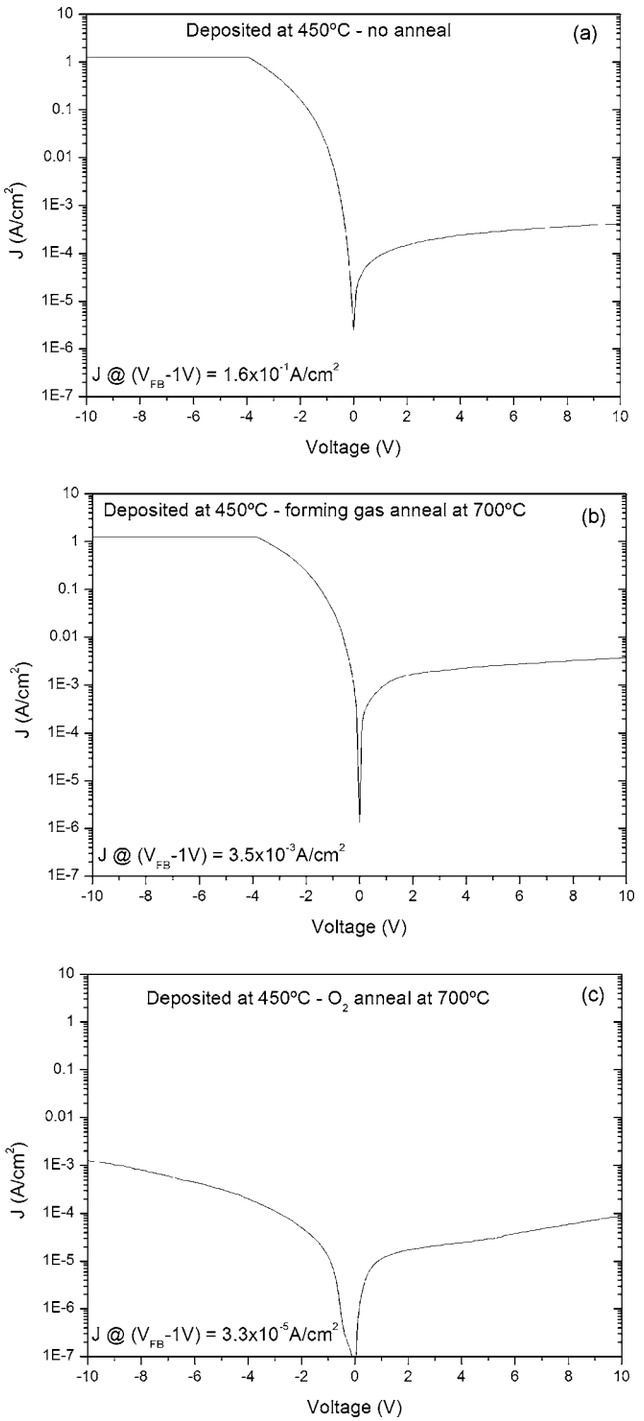

Figure 8. J-V plots of Hf silicate film deposited at 450°C for the (a)as-deposited film, (b) forming gas annealed film, and (c) O_2 annealed film.

this leakage current density value of 3.3×10^{-5} A/cm^2 for a resulting equivalent oxide thickness (EOT) of 8 nm following the O_2 anneal is approximately equivalent to that of a 2.6 nm SiO_2 film with a gate voltage of 1 V.[32] This high value of leakage current density in comparison with SiO_2 may be due to the presence of carbon impurities which remain in the film following the O_2 anneal for the 450°C deposition as well as metal impurities that may be present in the processing or annealing environments.[33] Likewise, slight decreases of impurity levels, interfacial oxide growth, and filling of oxygen vacancies[34] may also contribute to the decrease in leakage current observed for the hafnium silicate film annealed in O_2. Leakage mechanism plots for Poole-Frenkel [$\ln(J/E)$ vs $E^{1/2}$] and Schottky emission [$\ln(J)$ vs $E^{1/2}$][35] have been generated and the leakage behavior does not seem to strictly follow either type of mechanism. The presence of metal impurities from the processing environment as well as residual contamination from the metallorganic sources may also affect leakage, and should be considered as a potential leakage source. Ultimately, it is felt that the leakage observed both for the as-deposited and the annealed samples is most likely a combination of several different mechanisms (Poole-Frenkel, Schottky, ohmic), while Fowler-Nordheim emission and direct tunneling are unlikely because the films are not ultrathin and the electrical fields are relatively low.

Conclusions

In summary, a MOCVD process has been developed for the growth of hafnium silicate thin films using tetrakis(dimethylamino-)hafnium and tris(dimethylamino)silicon as source precursors with O_2 as a co-reactant. Si incorporation has been shown to increase with increasing deposition temperature, which is attributed to enhanced silicon source decomposition. The as-deposited Hf silicate films were observed to be amorphous and do not undergo crystallization at an annealing temperature up to 700°C in either forming gas or O_2 ambients. The effective dielectric constant was measured to be as high as 11.6 for films deposited at 450°C, and was observed to decrease after O_2 anneal, which is consistent with interfacial oxide growth. The leakage current density was also observed to show significant decrease after the high-temperature O_2 anneal. Accordingly, the tetrakis(dimethylamino)hafnium and tris(dimethylamino) silicon precursor source combination shows promise as a novel approach for the CVD growth of Hf silicate dielectrics.

Acknowledgments

This work was funded by the Semiconductor Research Corporation (SRC) and International SEMATECH under the Front End Processing Research Center (FEP-RC). This support is gratefully acknowledged.

The State University of New York at Albany assisted in meeting the publication costs of this article.

References

1. M. Tiezhong, S. A. Campbell, R. Smith, N. Hoilien, H. Boyong, H. C. Gladfelter, D. Buchanan, C. Taylor, M. Gribelyuk, M. Tiner, M. Coppel, and J. J. Lee, *IEEE Trans. Electron Devices*, **48**, 2348 (2001).
2. G. D. Wilk, R. M. Wallace, and J. M. Anthony, *J. Appl. Phys.*, **89**, 5243 (2001).
3. C.-L. Liu, Z. X. Jiang, R. I. Hedge, D. D. Sieloff, R. S. Rai, D. C. Gilmer, C. C. Hobbs, P. J. Tobin, and S. Lu, *Appl. Phys. Lett.*, **81**, 1441 (2004).
4. F. Lime, K. Oshima, M. Cassé, G. Ghibaudo, S. Cristoloveanu, B. Guillaumot, and H. Iwai, *Solid-State Electron.*, **47**, 1617 (2003).
5. H. Wong, N. Zhan, K. L. Ng, M. C. Poon, and C. W. Kok, *Thin Solid Films*, **462–463**, 96 (2004).
6. Y. S. Lin, R. Puthenkovilakam, and J. P. Chang, *Appl. Phys. Lett.*, **81**, 2041 (2002).
7. J. Robertson, *J. Vac. Sci. Technol. B*, **18**, 1785 (2000).
8. R. G. Gordon, J. Becker, D. Hausmann, and S. Suh, *Chem. Mater.*, **13**, 2463 (2001).
9. P. A. Williams, A. C. Jones, N. L. Tobin, P. R. Chalker, S. Taylor, P. A. Marshall, J. F. Bickley, L. M. Smith, H. O. Davies, and G. W. Critchlow, *Chem. Vap. Deposition*, **9**, 309 (2003).
10. X. Liu, S. Ramanathan, and T. E. Seidel, *Mater. Res. Soc. Symp. Proc.*, **765**, 97 (2003).
11. J.-H. Lee, J. P. Kim, J. -H Lee, Y.-S. Kim, H.-S. Jung, N.-I. Lee, H.-K. Kang, K. P. Suh, M.-M. Jeong, K.-T. Hyun, H.-S. Baik, Y. S. Chung, X. Liu, S. Ramanathan, T. Seidel, J. Winkler, A. Londergan, H. Y. Kim, J. M. Ha, and N. K. Lee, *Tech. Dig. - Int. Electron Devices Meet.*, **2002**, 221.
12. M. Cho, D. S. Jeong, J. Park, H. B. Park, J. Park, S. W. Lee, T. J. Park, C. S. Hwang, G. H. Jang, and J. Jeong, *Appl. Phys. Lett.*, **85**, 5953 (2004).
13. S. Hino, M. Nakayama, K. Takahashi, H. Funakubo, and E. Tokumitsu, *Jpn. J. Appl. Phys., Part 1*, **42**, 6015 (2003).
14. J. Schaeffer, N. V. Edwards, R. Liu, D. Roan, B. Hradsky, R. Gregory, J. Kulik, E. Duda, L. Contreras, J. Christiansen, S. Zollner, P. Tobin, B.-Y. Nguyen, R. Nieh, M. Ramon, R. Rao, R. Hedge, R. Rai, J. Baker, and S. Voight, *J. Electrochem. Soc.*, **150**, F67 (2003).
15. K. Takahashi, M. Nakayama, S. Yokoyama, T. Kimura, E. Tokumitsu, and H. Funakubo, *Appl. Surf. Sci.*, **216**, 296 (2003).

16. A. R. Teren, P. Ehrhart, R. Waser, J. Q. He, C. L. Jia, M. Schumacher, J. Linder, P. K. Baumann, T. J. Leedham, S. R. Rushworth, and A. C. Jones, *Integrated Ferroelectrics*, **57**, 1163 (2003).
17. K. Takahashi, H. Funakubo, S. Hino, M. Nakayama, N. Ohashi, T. Kiguchi, and E. Tokumitsu, *J. Mater. Res.*, **19**, 584 (2004).
18. Y. Ohshita, A. Ogura, A. Hoshino, S. Hiiro, T. Suzuki, and H. Machida, *Thin Solid Films*, **406**, 215 (2002).
19. A. Ogura, K. Ito, Y. Ohshita, M. Ishikawa, and H. Machida, *Thin Solid Films*, **441**, 161 (2003).
20. A. Deshpande, R. Inman, G. Jursich, and C. Takoudis, *J. Vac. Sci. Technol. A*, **22**, 2035 (2004).
21. K. Kukli, M. Ritala, T. Sajavaara, J. Keinonen, and M. Leskelä, *Chem. Vap. Deposition*, **8**, 199 (2002).
22. K. Kukli, M. Ritala, J. Lu, A. Harsta, and M. Leskelä, *J. Electrochem. Soc.*, **151**, F189 (2004).
23. D. Hausmann, E. Kim, J. Becker, and R. G. Gordon, *Chem. Mater.*, **14**, 4350 (2002).
24. T. Maruyama and T. Shirai, *Appl. Phys. Lett.*, **63**, 611 (1993).
25. K. Yasui, K. Otsuki, and T. Akahane, *J. Non-Cryst. Solids*, **169**, 301 (1994).
26. R. A. Levy, X. Lin, J. M. Grow, H. J. Boeglin, and R. Shalvoy, *J. Mater. Res.*, **11**, 1483 (1996).
27. T. Aoki, T. Ogishima, A. M. Wrobel, Y. Nakanshi, and Y. Hatanaka, *Vacuum*, **51**, 747 (1998).
28. M. Boudreau, M. Boumerzoug, P. Mascher, and P. E. Jessop, *Appl. Phys. Lett.*, **63**, 3014 (1993).
29. S. Kamiyama, T. Miura, Y. Nara, and T. Arikado, *Electrochem. Solid-State Lett.*, **8**, G215 (2005).
30. J. Zhu, Z. G. Liu, and Y. Feng, *J. Phys. D*, **36**, 3051 (2003).
31. V. Rangarajan, H. Bhandari, and T. Klein, *Thin Solid Films*, **419**, 1 (2002).
32. Y. Taur, *IBM J. Res. Dev.*, **46** (2/3), 213 (2002).
33. S. Skordas, F. Papadatos, S. Consiglio, E. T. Eisenbraun, and A. E. Kaloyeros, *J. Mater. Res.*, **20**, 1536 (2005).
34. O. Buiu, Y. Lu, I. Z. Mitrovic, S. Hall, P. Chalker, and R. J. Potter, *Thin Solid Films*, In press.
35. T. Hori, *Gate Dielectrics and MOS ULSIs*, p. 44, Springer-Verlag, Berlin (1997).